Optimisation of a roll-to-roll hot embossing process for fabrication of micro-pyramid structures in thermoplastic sheets

Luke Haponow[1,a)], Jeff Kettle[1,2] and John Allsop[3]

[1]School of Computer Science and Electronic Engineering, Bangor University, Dean Street, Bangor, Gwynedd, LL57 1UT

[2]James Watt School of Engineering, University of Glasgow, Glasgow

[2]Ultra Precision Structured Surfaces Ltd, OpTIC Centre, Ffordd William Morgan, St Asaph Business Park, St Asaph, Denbighshire, LL17 0JD

[a)] Electronic mail: eeu23b@bangor.ac.uk

Abstract

Reported is the manufacture and optimisation of inverted micro-pyramid cavity structures into thermoplastic sheets using roll-to-roll (R2R) embossing. To manufacture the master, an ultra-precision diamond machining (UPDM) method was applied to create seamless surface structures into a copper-coated hot embossing roller. Using the hot embossing process, the roller features were successfully transferred to 2mm thick polymethyl methacrylate (PMMA) sheets. Optimisation of the R2R control process variables was conducted using Taguchi's numerical methods, which showed the importance of roller temperature for successful pattern transfer. The work shows that our process allows for microstructures to be manufactured into extruded PMMA sheets in a continuous process.

I. INTRODUCTION

Fabrication of macro, micro and nano sized structures is achievable through various fabrication and manufacturing methods and is of vital importance in microfluidics, anti-reflective surfaces and anti-fouling surfaces as well as a number of other applications[1]. Injection molding, UV and thermal nanoimprint lithography and soft casting are popular examples for manufacturing of such desired structures. To increase throughput, integration of these processes into roll-to-roll (R2R) manufacturing is often researched to reduce the processing cost and increase the throughput[2,3] UV-R2R embossing has been reported much more often in the literature and consists of a UV-curable resist that is continuously deposited onto a substrate with suitable UV-adhesion properties[4], and is then fed between two pressing rollers, one of which has the desired replication structure. The substrate is simultaneously exposed to a UV source whilst between the rollers to cure the UV-resin. R2R hot embossing is an alternative method and has the advantage of lower cost thermoplastic substrates without the need for expensive UV-curable resins and is generally considered cheaper, as a high resolution dispensing unit and UV-source are not required[5,6]. For R2R hot embossing, the system requires elevated temperature so that the thermoplastics can be heated above their glass transition temperature (T_g), which reduces the polymer viscosity[7,8], and allows for the desired surface structures to be physically formed into the substrate. For example, Sohn et al.[9] investigated the fabrication of micro-line grating structure arrays in polycarbonate (PC) substrates, and found that the most successful embossing, with regards to the magnitude of embossed structure depth, was achieved at a temperature of 150°C (approx. 5°C above

T_g of PC), compared to results using 100 and 125°C. Frenkel et al.[10] found that additional heating of a belt-type mold in an extrusion roller imprinting process, improved the fidelity of replicated sawtooth micro-structures, whereby the mold was heated to 210°C. Li et al.[11] also reported greater embossed structure depth through increasing roller temperature in a R2R hot embossing system that fabricated micro-pyramid arrays in polyethylene terephthalate glycol (PETG) films. However, at the highest processing temperature, demolding issues and adhesion between the embossing roller and substrate were introduced. Furthermore, increasing embossing temperature up to a certain point can begin to have a negative impact on the quality of embossing with regards to pattern fidelity. The higher the embossing temperature, the larger the amount of cooling is required during demolding to maintain embossed microstructures. With insufficient cooling, polymer reflow may occur whereby the structures will begin to recover[12]. Therefore optimisation of the embossing process is critical for successful structure replication.

The method of fabricating the embossing mold is a critical element within a R2R hot embossing system. As hot embossing is a 'one-to-one' process, the ability to replicate structures with high fidelity is largely dependent on the mold. Fabrication methods can be separated into direct structuring methods (such as micro-machining or laser treatment processes) and lithography methods (such as E-beam and UV lithography)[13]. Furthermore, molds can be either fabricated directly on to the roller surface, or created with the use of a flexible mold, which is then wrapped around the roller. UPDM is a direct fabrication method, whereby structures are created through the removal of material using diamond cutting tools and various machining techniques. An UPDM system

incorporates multiple axis' with high resolution positional control in the nanometer range, high speed spindles, accurate workpiece and tool holding fixtures, temperature control and vibration suppression[14], all of which are essential components in the manufacture of precision-made micro and nano-sized structures. The main advantages of UPDM include very high accuracy and nanometric surface roughness of fabricated geometries[15], large area molds can be manufactured (>1m), and a wide variety of size and shape structures are possible. Some disadvantages include the cost of the machine components within an UPDM system is quite high, and additional workpiece material coatings may be required if the workpiece is made from ferrous metal, such as steel, due to the difficulty in avoiding significant tool wear in diamond machining of ferrous materials[14,16].

The application of UPDM for the fabrication of molds for replication processes has been previously reported. For example, Kirchberg et al.[17] combined an UPDM process with micro injection molding to fabricate a microlens array in PMMA and PS (Polystyrene). Furthermore, UPDM has been reported elsewhere for application in R2R-UV embossing of subwavelength gratings[18], and linear Fresnel lenses[19].

Although there are some reports on fabrication of micro-pyramid structures in thermoplastic films[11,20] through R2R hot embossing, there is little in the literature regarding the fabrication of inverted pyramidal structures and also on use of thick rigid substrates. By adopting cavity-like features, it is possible to produce larger, wider angle structures compared to those more commonly found in R2R hot embossing studies (for example, 70µm in height micro-pyramid structure[11]), more suitable for diffusive lighting applications. Without protruding surface features, further modification such as additional anti-glare or protective film coatings can also be easily applied. This work reports the

fabrication of these structures, in particular the optimisation of the embossing process so that they can be fabricated on to commercially available, rigid plastic sheeting. This represents an alternative method of manufacturing diffusive lighting panels.

II. EXPERIMENTAL SET UP AND METHODOLOGY

A. R2R Hot Embossing System

A custom R2R hot embossing system was manufactured with the capability of processing both thermoplastic films and sheets. The system is installed in UPS^2 Ltd laboratories in Anglesey, Wales, UK. Figure 1(a) presents a 2D diagram of the applied R2R hot embossing format, and a 3D CAD model of the designed system is shown in Figure 1(b). The main embossing components include two precision manufactured rollers. The lower roller, referred to as the embossing roller, is internally heated and temperature controlled with a surface mounted thermocouple. The microstructures were manufactured using UPDM methods, and the roller is directly driven by a three-phase motor with a high torque gearbox. The upper roller, referred to as the nip roller, is coated in a compliant ethylene propylene diene monomer (EPDM) rubber coating and connected to two pneumatic pistons either side through take-up bearing housings. This allows the upper roller to be pressed downwards on to a substrate that is fed through and embossed by the lower roller. The pneumatic pistons were individually controlled by separate pressure gauges, to account for any non-uniformity of pressure that may arise in the system. An infra-red pre-heat stage was used to apply a pre-heat treatment to substrates, before passing through nip position. Two arrays of long-wave ceramic elements, mounted

in reflective steel casings, were positioned above and below the substrate to apply even heat dosages to the top and bottom surface of the substrate to avoid any warping deformation.

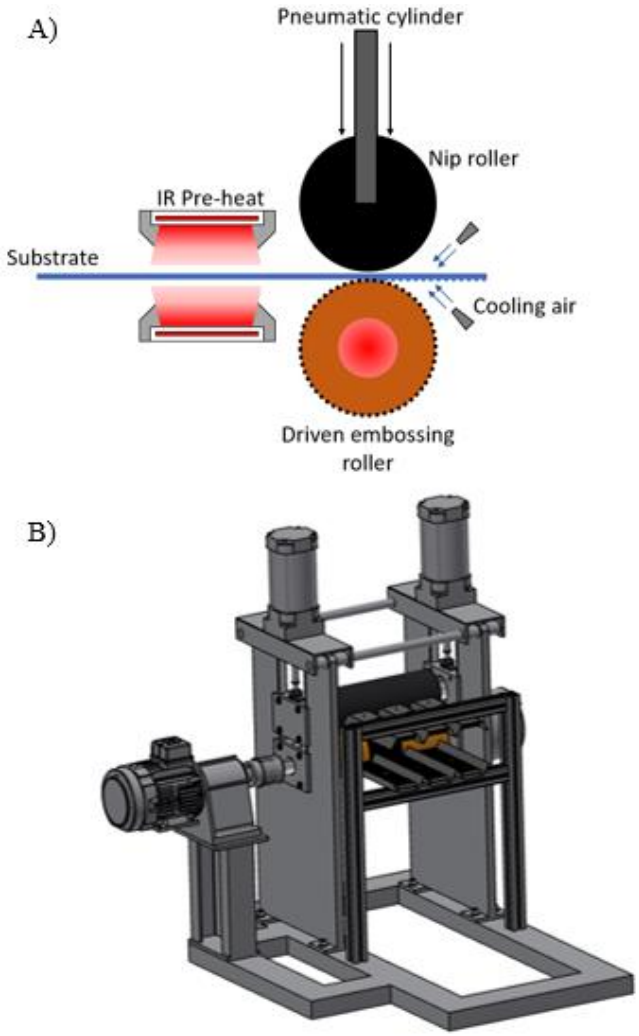

FIG. 1. A) 2D diagram of the applied R2R hot embossing system format, b) CAD model of the developed R2R hot embossing system, with the main machine components visible.

B. Embossing Mold Fabrication

The embossing mold in this study was fabricated by UPDM methods using a custom built system, which is sited at UPS^2 Ltd manufacturing facility in St Asaph,

Denbighshire, Wales. A steel-based roller (390mm web length, 120mm diameter) was coated with a 1.5mm thick copper layer, through an electroplating process. Copper was chosen due to its suitable material characteristics for the UPDM process[21]. Its relative softness (compared to other metals such as steel) reduces tool wear, and a high quality optical finish can be achieved because of the small and consistent grain structure[22]. When machining cylindrical components, seamless patterns can be fabricated[23], therefore a seam line once per revolution is not transferred to the embossed substrates, compared to other methods that involve wrapping a flexible mold around a cylindrical embossing component, that create a seam where the two ends of the wrapped mold meet[24].

An initial highly reflective, mirror-like surface was machined on the roller to allow the UPDM process of micro-structure fabrication, through the application of ultra-precision diamond turning (UPDT), reducing the surface roughness to an average of (R_A)<10nm and peak to peak surface roughness (R_Z)<200nm. Three-sided pyramids (or tetrahedrons) were fabricated, using a sharp V-grooved diamond cutting tool, positioned in hexagonal arrays and wrapped seamlessly around the roller circumference, with structure heights of less than 200µm. UPDM allows seamless structure fabrication due to the constant contact between the workpiece and diamond cutting tool during rotation. The diamond cutting tool was inspected during the machining process to ensure no significant tool wear had occurred, which would result in deterioration of the fabricated structure quality. A central section of the roller was fabricated with these structures, and afterwards further material either side of the pattern area was relieved to leave the microstructures as upstands. Figure 2 shows microscope images of the fabricated microstructures, and

Figure 3 shows an image of the manufactured embossing roller positioned on the R2R hot embossing system, coupled with the upper nip roller.

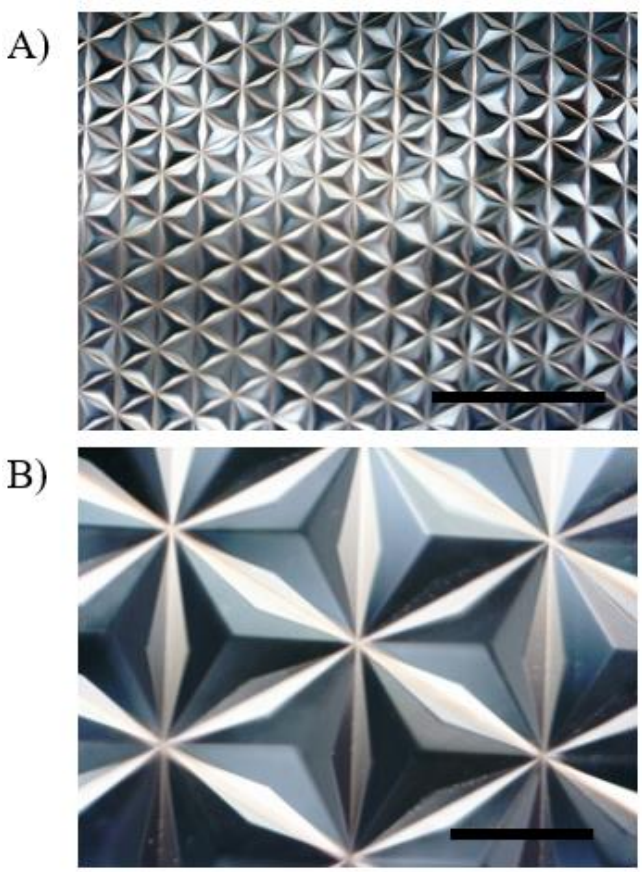

FIG. 2. USB microscope camera images of the UPDM micro-pyramid structures with a) low magnification image, scale bar = 3mm and b) high magnification image, scale bar = 0.5mm.

FIG. 3. Image of the fabricated microstructure mold positioned on the R2R hot embossing system.

C. Embossing Experiments Design

R2R hot embossing experiments were conducted using a Design of Experiment (DoE) method based upon a Taguchi orthogonal array. This involves the application of highly fractional orthogonal arrays that allow the experiment designer to significantly reduce the number of required experimental runs, but maintain balanced experimental data that investigates each experiment variable equally. Embossing roller temperature, pre-heat temperature and nip roller pressure were all chosen as experiment variables, as the temperature and pressure which thermoplastics are embossed with has proven to be influential in the quality and pattern fidelity of embossed substrates[13]. Although drive speed is also an important hot embossing parameter, it was fixed at 0.5rpm for the experiments, as changing the speed would affect the applied dosage of pre-heat treatment for a given temperature. In initial experiments conducted on the system, which included variation of the drive speed (0.5, 1.0 and 2.0rpm), 0.5rpm was found to be the most

successful speed for embossing results, hence this value was chosen for the experiment reported herein. This speed was also set as the minimum setting because when drive speed slower than 0.5rpm was applied, significant 'warping' was present in the PMMA substrates. Taguchi's $L_9(3^3)$ array was chosen for the experiments, with the parameter values are shown in Table I.

TABLE I. Parameter values for the R2R hot embossing experiments undertaken in this study.

Control Factor		Level 1	Level 2	Level 3
A	Roller Temperature (°C)	105	110	115
B	Pre-heat Temperature (°C)	160	180	200
C	Pressure (bar)	3	4	5

Commercially available 2mm thick PMMA sheets, which were sourced from Plastock UK, were used as the embossing substrate. The glass transition temperature was approximately 105°C[25,26]. Dimensional values of the embossed structures in all fabricated samples were measured by microscope imaging, before converting into a percentage of the original mold structure dimension, referred to as the 'fill factor %'. These results were to be used for the response values for Taguchi's analysis.

III. RESULTS AND DISCUSSION

Microscope images presenting all 9 fabricated samples from the $L_9(3^3)$ experiment are shown in the photo array in Figure 4, with the corresponding calculated fill factor % for each sample shown in Table II. The values of all embossing parameters for each experimental run are also shown in Table II. The microscope imaging software was used to measure the embossed feature dimensions. The signal-to-noise ratios (SNR) calculated for each variable level from Taguchi's analysis of the hot embossing experiments using the statistical software, Minitab, are presented in Table III, with the values plotted in Figure 5(a). The values were calculated with the fill factor % used as the response parameter, measured from the sample images in Figure 4. In Taguchi's analysis, the SNR allows us to investigate the quality characteristics of variables, by taking a ratio of calculated signal power (i.e. the predictable part of a process output) and noise power (i.e. the unpredictable part). The calculation of the SNR depends on the desired effect on the system response . In this study, maximization of the fill factor % was the target, therefore the 'larger-is-better' characteristic was selected for analysis, with the equation used shown in Eq. (1),

$$SNR = -10\log\left(\frac{1}{n}\sum_{i=1}^{n}\frac{1}{y_i^2}\right) \quad (1)$$

where n represents the number of samples per run and y_i is the measured response.

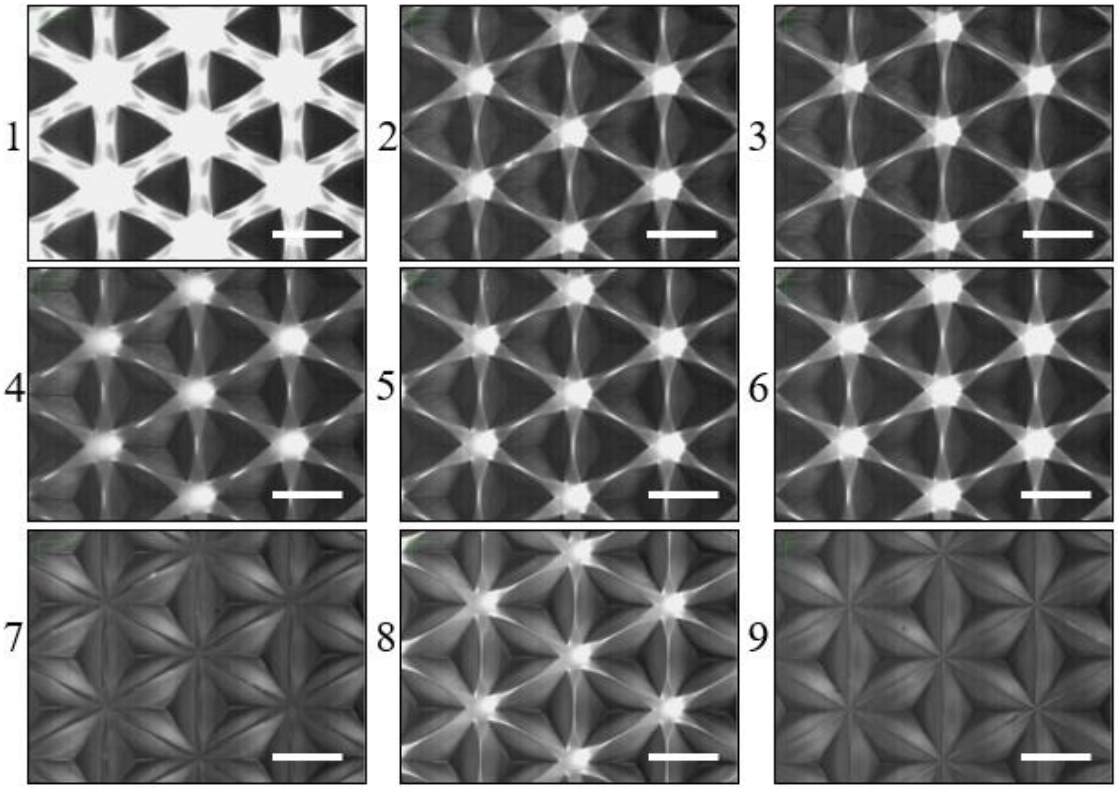

FIG. 4. Microscope images taken of all 9 embossed samples, scale bar = 500μm.

Larger SNR values shown in Table III and Figure 5(a), show greater impact on the measured response. Table III also shows the difference between the minimum and maximum values for each main effect. It can be concluded from the Taguchi's analysis results, that within the range used, increasing roller temperature, pre-heat temperature and pressure all improve the embossed pattern fidelity. Therefore, the optimum conditions in this experiment for hot embossing are roller temperature of 115°C, pre-heat temperature of 200°C and pressure of 5bar.

TABLE II. Experiment data for each run and the calculated response from the microscope images taken of all 9 embossed samples.

Experiment Number	Roller Temperature (°C)	Pre-heat Temperature (°C)	Pressure (bar)	Fill Factor (%)
1	105	160	3	50.7
2	105	180	4	61.3
3	105	200	5	67.1
4	110	160	4	60.1
5	110	180	5	70.9
6	110	200	3	60.3
7	115	160	5	80.4
8	115	180	3	68.2
9	115	200	4	95

TABLE III. Signal-to-noise ratios for the R2R hot embossing experiments undertaken in this study.

Level	Roller Temperature (°C)	Pre-heat Temperature (°C)	Pressure (bar)
1	35.32	35.77	35.32
2	35.96	36.41	36.88
3	38.03	37.15	37.12
Δ	2.71	1.38	1.8

It is also evident that an increase in roller temperature, particularly from 110 to 115°C, had the greatest effect on the fill factor %, over the experimental range chosen. This is shown by the delta value in Table III, and quite clearly in the SNR plot of roller temperature in Figure 5(a). Furthermore, full replication is shown in sample 9, and near-full replication is shown in samples 7 and 8, in Figure 4. In each of these 3 experiments, roller temperature was set at 115°C. Even without optimum conditions (i.e. maximum values in all 3 variables), pattern fidelity was high when using a roller temperature of 115°C.

Further analysis was carried out to investigate any process variable interaction, as well as the significance of each variable, through analysis of variance (ANOVA). Figure 5(b) and 5(c) summarize the results, with a half normal probability plot and pareto chart. The standardized effects of variables are used in both plots. Using standardized effects rather than simple effects allows us to compare variables that have different units, by removing the units when calculating the effect. Therefore, direct comparison of the standardized effects of temperature against pressure can be made. The absolute standardized effect is plotted on the half normal plot, therefore only the magnitude of the effect, and not the direction, is shown.

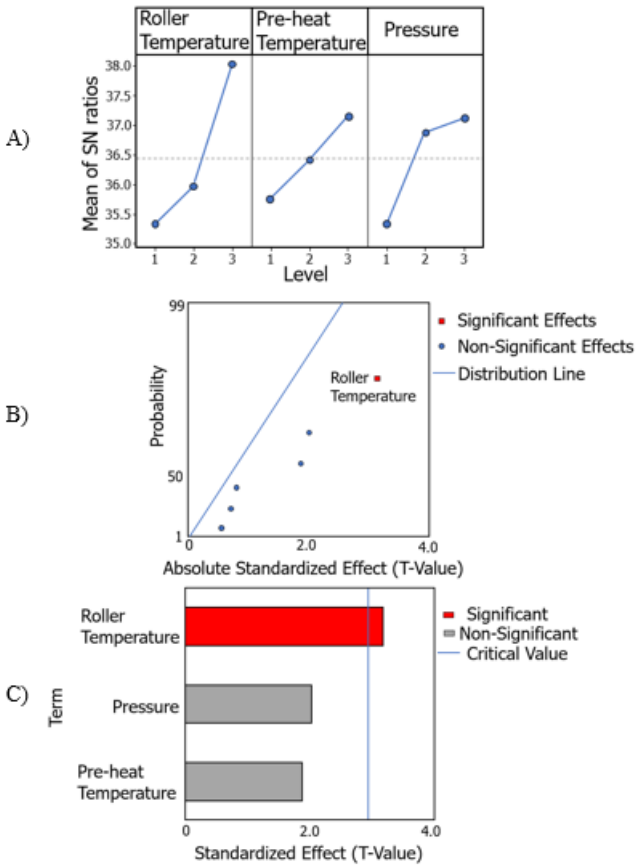

FIG. 5. A) Signal-to-noise ratios plotted against factor levels for all three tested parameters, B) Half normal probability plot from ANOVA, C) Pareto chart from ANOVA.

In a half normal probability plot, variables that do not follow the normal distribution, and are distanced to the right and below the line of best fit, show larger effect on the measured response[27]. By contrast, the pareto chart shows the effects of variables with reference to a critical value, illustrated with a vertical reference line, which indicates the statistical significance of each process variable. Using both plots, it is possible to deduce that the roller temperature has the most significant effect on the experiment response, but also that the pre-heat temperature and pressure are not statistically significant, i.e. they were not found to reject the null hypothesis within the

processing window that is investigated. This is shown by considering the deviation from the normal distribution line in the probability plot, and the T-value not being greater than the critical value line in the pareto chart, which was undertaken at an alpha level of 0.1. It is also noted, no interactions were found to have a significant effect on the embossed fill factor % (shown by blue points on the half normal plot in Figure 5(b)).

It is particularly interesting to note that the value of embossing temperature used was not significantly above the T_g of the PMMA substrate. It is common to use embossing temperatures 20°C and higher above the T_g of the substrate[28,29] to achieve good quality embossed substrates with high pattern fidelity. However some studies have shown that with the addition of a pre-heat treatment, lower temperatures just above the T_g can be successful in R2R hot embossing[30], this work shows that temperatures close to the T_g value can still enable successful pattern transfer. This is particularly impressive for an extruded PMMA sheet as polymer molecular weight is likely to be very high and thus is expected to have high polymer entanglement.

Using the optimised processing conditions, it was confirmed that full replication of the embossing mold features was achieved. An image of an embossed sheet from the system using the optimised processing conditions is shown in Figure 6(a), with a corresponding SEM image shown in Figure 6(b). The diffusive properties are clearly shown here, compared to the non-structured area of the thermoplastic sheet. When measuring the transmittance of the embossed sheet, a marginal improvement of approximately 1.2% was measured at 660nm, most likely as a result of enhanced coupling of light. However the diffusive properties were enhanced substantially. When

using a collimated 2” white light beam at the center of the substrate, the light output at a 60% normal to the substrate increased by 1005%, demonstrating its diffusive properties.

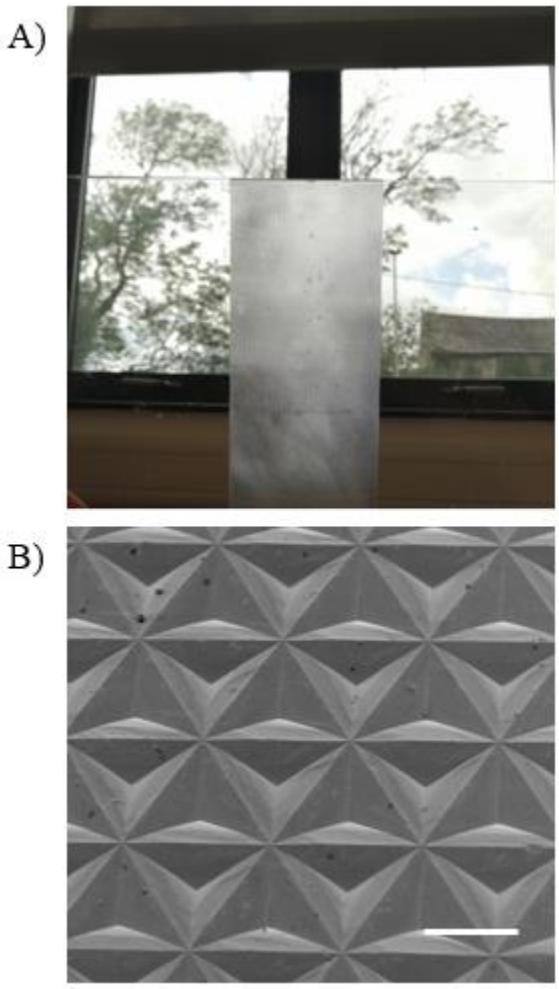

FIG. 6. A), Image of an embossed plastic sheet using the optimised R2R hot embossing parameters, B) SEM image of the embossed sample (45° angle, scale bar = 500µm).

IV. SUMMARY AND CONCLUSIONS

Reported is the optimisation of a R2R hot embossing process using a custom-built system that incorporates an UPDM patterned roller to create a seamless hot embossing mold consisting of inverted micro-pyramid array structures. We have used Taguchi’s

orthogonal arrays to optimise processing conditions, which significantly reduced the number of required experiments (reduction from 27 to 9 when comparing to full factorial methods for an experiment with the same number of variables and levels). On completion of the experiments, Taguchi's analysis and ANOVA was undertaken and found that the roller temperature used during processing was the most influential embossing parameter. When a roller setpoint of 115°C was applied, the SNR was maximized, and helped achieve full replication of structures even when pre-heat temperature and pressure were both not set to their optimum values found through Taguchi's analysis. Using the optimised process, patterns were successfully transferred to 2mm thick PMMA sheets, making them suitable for diffusive lighting panel applications, which often require more complex and expensive extrusion-based systems for manufacture in this application.

ACKNOWLEDGMENTS

The authors gratefully acknowledge the financial support provided by the Knowledge Economy Skills Scholarships (KESS 2, Ref: BUK2121).

[1]M. Heckele and W.K. Schomburg, J. Micromechanics Microengineering **14**, (2004).

[2]H.N. Hansen, R.J. Hocken, and G. Tosello, CIRP Ann. - Manuf. Technol. **60**, 695 (2011).

[3]S. Lan, H. Lee, J. Ni, S. Lee, and M. Lee, in *ICSMA 2008 - Int. Conf. Smart Manuf. Appl.* (IEEE, 2008), pp. 371–376.

[4]H. Lan and Y. Ding, in *Lithography* (InTech, 2010), pp. 1–8.

[5]H. Lan, in *Micro/Nanolithography - A Heuristic Asp. Endur. Technol.* (InTech, 2018), p. 29.

[6]J.J. Dumond and H. Yee Low, J. Vac. Sci. Technol. B, Nanotechnol. Microelectron. Mater. Process. Meas. Phenom. **30**, 010801 (2012).

[7]N. Kodihalli Shivaprakash, T. Ferraguto, A. Panwar, S.S. Banerjee, C.F. Barry, and J. Mead, ACS Omega **4**, 12480 (2019).

[8]L.J. Guo, J. Phys. D. Appl. Phys. **37**, (2004).

[9]K.J. Sohn, J.H. Park, D.E. Lee, H.I. Jang, and W. Il Lee, J. Micromechanics Microengineering **23**, (2013).

[10]R. Frenkel, B. Kim, and D. Yao, Machines **2**, 299 (2014).

[11]W. Li, Y. Zhai, P. Yi, and Y. Zhang, Microelectron. Eng. **164**, 100 (2016).

[12]S.H. Ng and Z.F. Wang, DTIP MEMS MOEMS - Symp. Des. Test, Integr. Packag. MEMS/MOEMS 262 (2008).

[13]L. Peng, Y. Deng, P. Yi, and X. Lai, J. Micromechanics Microengineering **24**, (2014).

[14]M. Roeder, T. Guenther, and A. Zimmermann, Micromachines **10**, (2019).

[15]E. Brinksmeier, R. Gläbe, and L. Schönemann, CIRP J. Manuf. Sci. Technol. **5**, 1 (2012).

[16]L. Zou, J. Yin, Y. Huang, and M. Zhou, Diam. Relat. Mater. **86**, 29 (2018).

[17]S. Kirchberg, L. Chen, L. Xie, G. Ziegmann, B. Jiang, K. Rickens, and O. Riemer, Microsyst. Technol. **18**, 459 (2012).

[18]C.-W. Liu, J. Yan, and S.-C. Lin, Opt. Eng. **55**, 064105 (2016).

[19]X. Zhang, K. Liu, X. Shan, and Y. Liu, Opt. Express **22**, A1835 (2014).

[20]L. Lin, T.K. Shia, and C.J. Chiu, J. Micromechanics Microengineering **10**, 395 (2000).

[21]T. Moriwaki, CIRP Ann. - Manuf. Technol. **38**, 115 (1989).

[22]S.J. Zhang, S. To, S.J. Wang, and Z.W. Zhu, Int. J. Mach. Tools Manuf. **91**, 76 (2015).

[23]X. Zhang, R. Huang, K. Liu, A.S. Kumar, and X. Shan, Precis. Eng. **51**, 445 (2018).

[24]A. Rank, V. Lang, and A.F. Lasagni, Adv. Eng. Mater. **19**, 1 (2017).

[25]S. Kim, Y. Son, H. Park, B. Kim, and D. Yun, 164 (2015).

[26]H. Mekaru and H. Hiroshima, Jpn. J. Appl. Phys. **52**, (2013).

[27]K. Esbensen, B. Swarbrick, F. Westad, P. Whitcomb, and M. Anderson, *Multivariate Data*

Analysis: An Introduction to Multivariate Analysis, Process Analytical Technology and Quality by Design (2018).

[28]K. Metwally, S. Queste, L. Robert, R. Salut, and C. Khan-Malek, Microelectron. Eng. **88**, 2679 (2011).

[29]Y. Deng, P. Yi, L. Peng, X. Lai, and Z. Lin, J. Micromechanics Microengineering **24**, (2014).

[30]L.P. Yeo, S.H. Ng, Z.F. Wang, H.M. Xia, Z.P. Wang, V.S. Thang, Z.W. Zhong, and N.F. De Rooij, J. Micromechanics Microengineering **20**, (2010).